[2123] 地震力を受けるRC柱・はり接合部のせん断抵抗機構に関する解析的研究

ANALYTICAL STUDY ON SHEAR RESISTANCE MECHANISMS OF RC BEAM-COLUMN JOINTS SUBJECTED TO SEISMIC FORCES

Hiroshi NOGUCHI* and Kazuhiro WATANABE*

1. INTRODUCTION

There have been many active experimental studies for beam-column joints, but it is necessary to investigate the nonlinear behaviour of beam-column joints analytically in order to clarify the shear resistance mechanisms and develop a rational design method for beam-column joints. Therefore, in this study, the nonlinear behaviour of beam-column joints under reversed cyclic loading was analyzed by the FEM (1), (2), (3). An investigating approach in this study is shown in Fig. 1. Reflecting that previous finite element analyses have been used rather complementally for the investigation of test results, the change of stress flow in joint concrete is investigated from FEM analytical data in detail. Shear forces contributed by concrete and shear reinforcing bars are calculated from the FEM analytical data and they are compared with shear forces contributed by the corresponding components of the previous macro model.

2. ANALYTICAL MODELS

The subject of analysis was limited to the joint without transverse beams, and the plane stress was assumed. In this FEM model, the rotation of principal axes and the stress-strain curves of concrete under cyclic stresses, the criterion for opening and closing of a crack and the bond stress-slip curves under cyclic stresses were considered. These analytical models are especially important in the FEM analysis dealing with shear and bond behaviour of R/C members under reversed cyclic loading. The development process for the analytical models was written in Ref. (2).

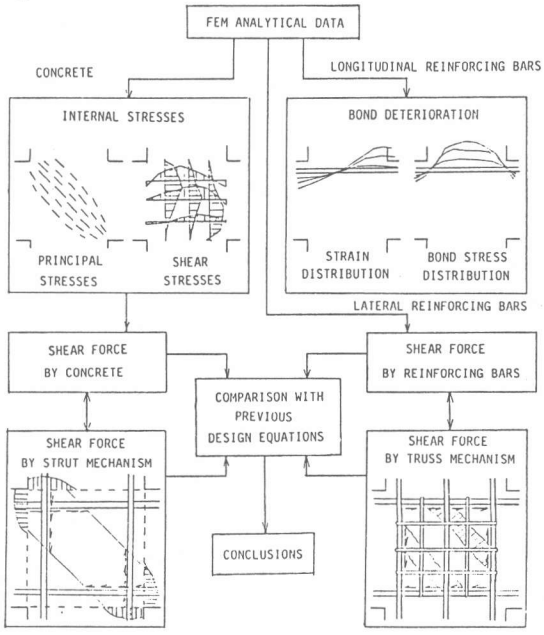

Fig. 1 Investigating Approach

* Department of Architectural Engineering, Chiba University

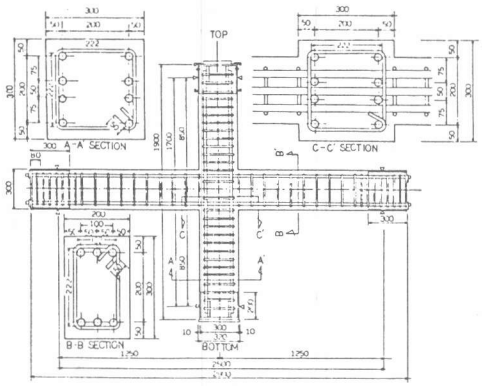

Fig. 2 Detail of Specimen

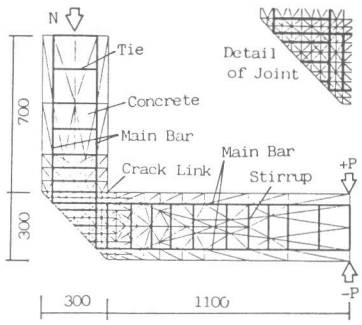

Fig. 3 Finite Element Idealization

3. SPECIMENS TO BE ANALYZED

Four half-scaled interior joint specimens, J - 1, J - 1', J - 2 , J - 3, were selected for the subject of analysis as shown in Table 1. Specimen J - 1 was tested by Kamimura and Hamada (4), and specimens J - 2 and J - 3 were tested by Tada and Takeda (5). Each specimen had its own failure mode as shown in Table 1. The middle longitudinal reinforcing bars were set up only in the column of an imaginary specimen J - 1' to study the role of the column middle reinforcing bars in the shear resistance of a joint with good bond for beam longitudinal bars.

Table 1 Specimens and Material Properties

Specimen	J-1	J-1'	J-2	J-3
Failure Mode	Joint Failure Bond Deterioration	Joint Failure	Bond Deterioration after Beam Yielding	Beam Yielding
Bond of Beam Bars	Poor	Good	Poor	Perfect
Concrete	E_0 = 2.54 $\times 10^5$ kgf/cm^2 f_c = 197 kgf/cm^2		E_0 = 2.20 $\times 10^5$ kgf/cm^2 f_c = 290 kgf/cm^2	
Longitudinal Bars	E_s = 1.94 $\times 10^6$ kgf/cm^2 $_s\sigma_y$ = 3633 kgf/cm^2		E_s = 2.11 $\times 10^6$ kgf/cm^2 $_s\sigma_y$ = 3510 kgf/cm^2	
Stirrups and Ties	E_s = 1.98 $\times 10^6$ kgf/cm^2 $_s\sigma_y$ = 3300 kgf/cm^2		E_s = 2.11 $\times 10^6$ kgf/cm^2 $_s\sigma_y$ = 3200 kgf/cm^2	
Bond Characteristic (Analytical)	Initial Bond Stiffness = 8000 kgf/cm^3 Second Bond Stiffness = 400 kgf/cm^3			
	σ_{b1} = 21 kgf/cm^2 σ_{b2} = 50 kgf/cm^2	σ_{b1} = 60 kgf/cm^2 σ_{b2} =120 kgf/cm^2	σ_{b1} = 28 kgf/cm^2 σ_{b2} = 60 kgf/cm^2	σ_{b1} = 84 kgf/cm^2 σ_{b2} =180 kgf/cm^2
Beam Top&Bottom Bars Pt(%) Stirrups Pw(%)	3-D22 (SD35) 2.32 2-9ϕ @10.0 0.64	9 D13 (SD35) 2.32 2-9ϕ @10.0 0.64	3-D16 (SD30) 1.19 2-9ϕ @15.0 0.42	3-D16 (SD30) 1.19 2-9ϕ @15.0 0.42
Column Total Bars Middle Bars Pg(%) Hoops Pw(%)	8-D22 — 3.44 2-9ϕ @6.0 36.0	10-D22 (2-D22) 4.30 2-9ϕ @6.0 36.0	8-D16 — 1.77 2-9ϕ @10.0 45.0	8-D16 — 1.77 2-9ϕ @10.0 45.0
Connection Hoops Set&Space Pw(%)	2-9ϕ 3set @6.0 0.58	2-9ϕ 3set @ 6.0 0.58	2-9ϕ 5set @ 4.0 0.98	2-9ϕ 5set @ 4.0 0.98

*) σ_{b1} : Bond Deteriolation Stress σ_{b2} : Maximum Bond Stress

The detail and the finite element idealization of the specimens are shown in Figs. 2 - 3, respectively. The crack pattern was set up using link elements in accordance with the test results. In the analysis, two and half cycles of reversed deflection were applied to specimens J - 1, J - 2, J - 3 except for specimen J - 1'.

4. RESTORING FORCE CHARACTERISTICS

The analytical load-story displacement relationships are compared with the test results in Fig. 4. For J - 1 and J - 2, the analytical results gave good agreement with the experimental shape of hysteresis loops. The analytical restoring force characteristics adopted the pinching shape with poor energy dissipation capacity, as cracking and bond deterioration of beam longitudinal bars in the joint progressed under the subsequent cyclic loading. For specimen J - 3, the analytical restoring force characteristics showed the stable spindle-shape hysteresis loops and almost the same tendency as the test results. For specimen J - 1' with good bond for beam longitudinal bars, the analytical maximum strength was higher than the experimental strength for specimen J - 1 with poor bond. For J - 1, J - 2, J - 3, the analytical results also gave a good

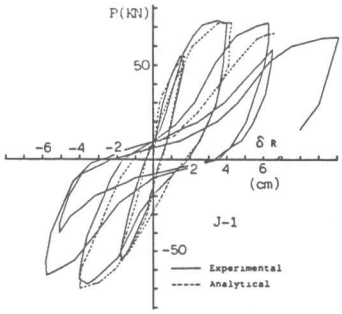

a) Shear and Bond Deterioration (J - 1)

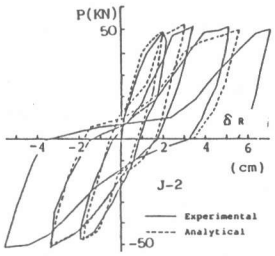

b) Bond Deterioration after Beam Flexural Yielding (J - 2)

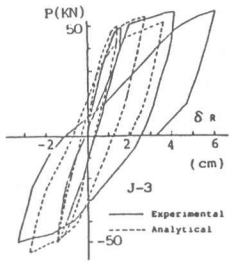

c) Beam Flexural Yielding (J - 3)

Fig. 4 Load-Story Displacement Relationships

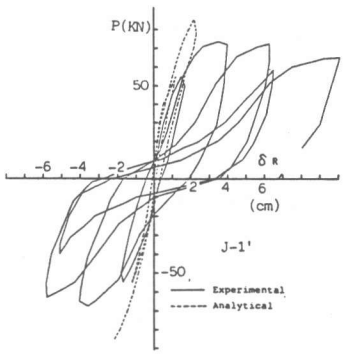

Fig. 4 d) Shear Deterioration (J - 1')

agreement with the test results for crack propagation, progress of failure, joint behaviour, bond slip of beam longitudinal bars through the joint. The accuracy of the analytical results were considered to be sufficient to simulate the internal stresses in the joint.

5. PRINCIPAL STRESS DISTRIBUTION

Fig. 5 shows principal stress distribution of the joint concrete at the maximum strength for specimens J - 1, J - 1', and at the peak load during the last loading cycle for specimens J - 2, J - 3. It is one of the most distinctive points in FEM analysis that internal stress flow is visible. The compressive strut, where the compressive principal stress was dominant, was formed along the diagonal line of the joint near the peak load of each loading cycle. High compressive principal stress flowed more widely in the joint for good bond specimen, J - 3, than in the joint for bond deterioration type specimen, J - 2. The clear compressive strut was formed along the diagonal line for J - 1'. The stress strain of concrete after peak stress is represented by descendant slope called strain-

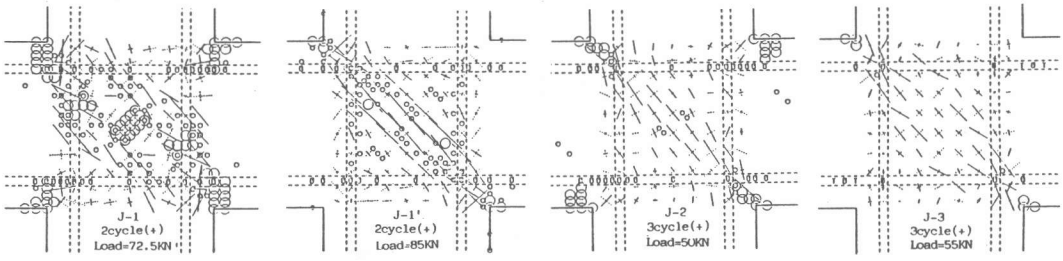

∘ : Strain Softening

○ : Compression Failure

○ : Bond Failure

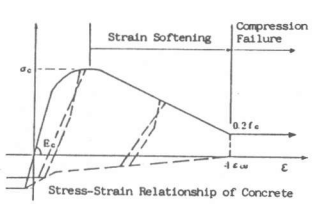

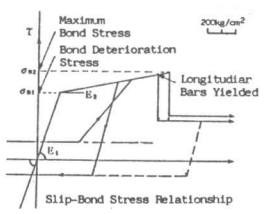

Fig. 5 Principal Stresses

softening which shows the behaviour in-between ductile and brittle state. Strain-softening was remarkable along the diagonal line on the joint of J - 1', but the compression failure was less remarkable in specimen J - 1' than in J - 1. The analytical failure mode gave a good agreement with the test results for specimens, J - 1, J - 2 and J - 3.

6. SHEAR STRESSES CONTRIBUTED BY COMPRESSIVE STRUT MECHANISM

The macro model for the shear resistance mechanisms proposed by Park and Paulay (6) was shown in Fig. 6. In the proposed macro model, the contribution of the concrete and joint reinforcing bars to the joint shear resistance were represented by the compressive strut mechanism and the truss mechanism, respectively. The horizontal joint shear force, V_{ch}, provided by the compressive strut mechanism was calculated from the corresponding FEM analytical data as follows,

$$V_{ch} = {}_BC_c + \Delta_B T_c - V_{col} \qquad (1)$$

in which ${}_BC_c$ = concrete compressive force from the beam, $\Delta_B T_c$ = part of the total beam bar force contributing to the strut mechanism and V_{col} = horizontal shear force across a column (See Fig. 6). In the shear stress distribution model, the shear forces contributed by compressive strut were obtained by integrating the concrete shear stress over the central horizontal section in the joint and subtracting the horizontal component of the diagonal reactin forces, which were made in joint concrete by the truss mechanism of joint reinforcing bars. The shear forces, V_{ch}, calculated by Eq. 1 are compared for the peak load in each cycle with the shear forces obtained by the shear stress distribution model in Fig. 7. The strut mechanism model gave a good agreement with the shear stress distribution model for all four specimens. It was shown that the

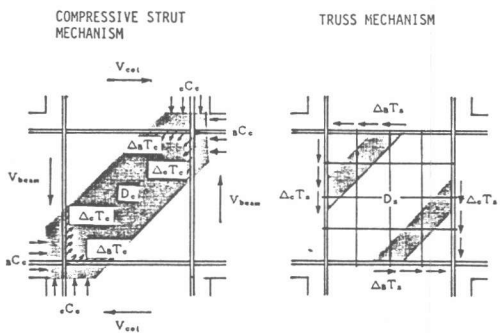

Fig. 6 Macro Model for Shear Resistance Mechanisms Proposed by Park and Paulay

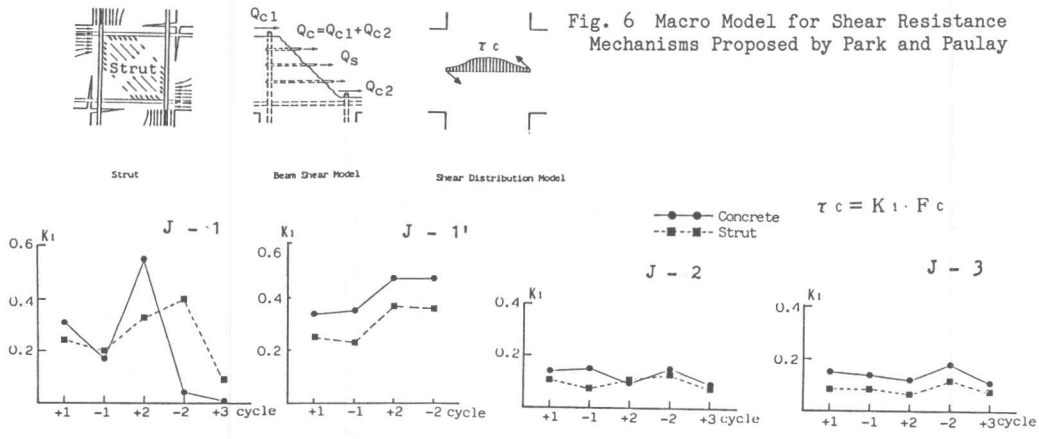

Fig. 7 Concrete Shear Stresses Calculated by Strut Mechanism and Shear Distribution Models

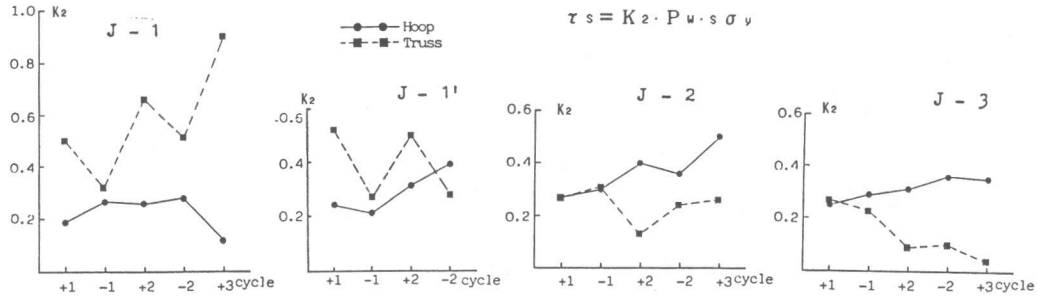

Fig. 8 Shear Stresses Calculated by Truss Mechanism and Strains in Joint Reinforcing Bars

shear stress contributed by concrete could be estimated by the compressive strut mechanism.

7. SHEAR STRESSES CONTRIBUTED BY TRUSS MECHANISM

The horizontal shear forces, V_{sh}, contributed by the truss mechanism was calculated from the FEM analytical data as follows,

$$V_{sh} = \Delta_B T_s \qquad (2)$$

in which $\Delta_B T_s$ = shear forces introduced at the boundaries of the joint core by beam bar bond forces in the outer concrete of the compressive strut (See Fig. 6). The shear forces, V_{sh}, calculated by Eq. 2 were compared for the peak load in each cycle with the shear forces obtained by the strain in the joint reinforcing bars in Fig. 8. The truss model was not in agreement with the contribution of joint reinforcing bars for J - 1, J - 2, J - 3. It was considered that this was because these three specimens had no middle longitudinal bars in the column, and the beam bar bond forces, T, in the joint were separated into the following two kinds; one is $\Delta_B T_c$ inside the compresive strut, and the other is $\Delta_B T_s$ outside the strut. In the Paulay and Park's truss mechanism model, the horizontal and vertical compression forces which need to be applied to the core concrete at the boundaries of the joint, to sustain the diagonal compression field , D_s in Fig. 6, can originate from distributed horizontal (joint shear reinforcing bars) and vertical tension reinforcement (column middle bars). For J - 1' with the column middle bars, the truss model gave a better agreement with the contribution of the joint reinforcing bars. It is considered that the further investigation is needed for the role of the column middle bars and the bond forces of the beam and column bars inside and outside of the compressive strut in the truss mechanism.

8. TOTAL SHEAR FORCES CONTRIBUTED BY CONCRETE AND SHEAR REINFORCING BARS

The total of shear forces contributed by concrete and joint reinforcing bars was calculated by the three method (Fig. 7) for specimen J - 1 as shown in Fig. 9. The two mechanisms (strut and truss) model gave a good agreement with the shear stress distribution model and the beam shear model for the specimen J - 1, which was of joint failure and bond deterioration type. But one should note that the errors in the strut and truss mechanism were compensated each other in the two mechanism model.

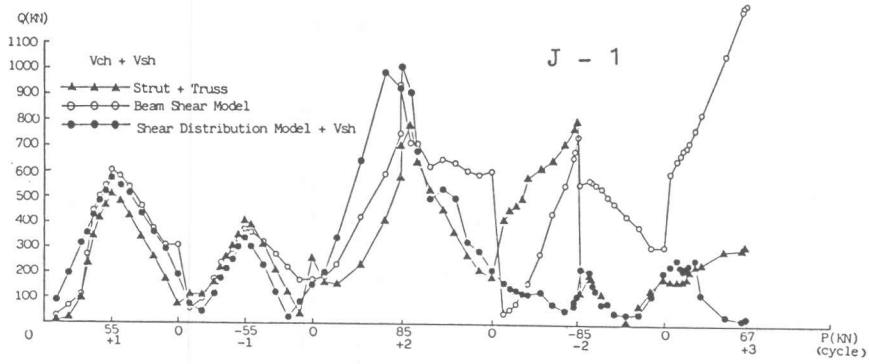

Fig. 9 Shear Forces Contributed by Concrete and Joint Reinforcing Bars

After the positive peak load in the second cycle, the good correspondence with the other two models could not be observed because of the local compression failure of joint concrete.

9. CONCLUSIONS

The nonlinear behaviour of reinforced concrete beam-column joints under reversed cyclic loading was analyzed by the FEM with the emphasis on the shear resistance mechanisms of a joint.

The shear forces contributed by joint concrete could be estimated by the compressive strut mechanism model proposed by Park and Paulay considerably well.

The truss model proposed by Park and Paulay was not in agreement with the contribution of joint reinforcing bars for the specimens without the middle longitudinal bars in the column. The further investigation is needed for the role of each component of the truss model.

REFERENCES

1. Noguchi, H., "Nonlinear Finite Element Analysis of Beam-Column Joints," Final Report, IABSE Colloquium on Advanced Mechanics of Reinforced Concrete, Delft, 1981, pp. 639-654.
2. Noguchi, H., "Analytical Models for Cyclic Loading of Reinforced Concrete Members," Finite Element Analysis of Reinforced Concrete Structures, Proc. of the Japan-U.S. Seminar in Tokyo, May 1985, ASCE, 1986, pp. 486-506.
3. Noguchi, H. and Naganuma, K., "Nonlinear Finite Element Analysis of Restoring Force Characteristics of Reinforced Concrete Beam-Column Joints," Proc. of the Eighth World Conf. on Earthquake Engrg., San Francisco, July 1984, pp. 543-550.
4. Kamimura, T., et al., "Experimental Study on Reinforced Concrete Beam-Column Joints, Part 1-3," Proc. Annual Conv., AIJ, Sept. 1978, pp. 1673-1674, Sept. 1979, pp. 1303-1306 (in Japanese).
5. Tada, T., Takeda, T. and Takemoto, Y., "Experimental Study on the Reinforcing Method of RC Beam-Column Joints," Proc. Kanto District Symp., AIJ, July 1976, pp. 225-236 (in Japanese).
6. Paulay, T. and Park, R., "Joints in Reinforced Concrete Frames Designed for Earthquake Resistance," A Report Prepared for the U.S.-New Zealand-Japan Seminar, Monterey, California, August 1984, pp. 16-18.